

## "Processing and Characterization of SALDVI Ceramic Structures"

James E. Crocker, Lianchao Sun, Helene Ansquer, Leon L. Shaw, and Harris L. Marcus  
Institute of Materials Science  
University of Connecticut

### Abstract

Selective Area Laser Deposition Vapor Infiltration (SALDVI) ceramic structures and composites are fabricated by the localized chemical vapor infiltration of powder layers. A matrix of vapor deposited ceramic material is selectively deposited from gas precursors into a bed of ceramic powder particles using laser heating. An important aspect of the SALDVI process for building 3-D structures is the depth of penetration of the infiltration zone into the powder layer. The infiltration behavior of vapor deposited silicon carbide from tetramethylsilane gas was investigated for a range of ceramic powders with different optical, thermal, and physical properties using image analysis. The porosity distribution in the silicon carbide matrix SALDVI structure was found to vary with particle size and particle material. These results will be used to guide experiments on the effect of layer thickness on the microstructure of multiple layer SALDVI composites.

### Introduction

Selective Area Laser Deposition Vapor Infiltration (SALDVI) is a developing Solid Freeform Fabrication technique for fabricating, using a layer-by-layer approach, ceramic and composite structures and multiple material shapes containing embedded devices<sup>1-4</sup>. By the process of chemical vapor deposition (CVD), a matrix of solid material is deposited from a gas precursor into a layer of ceramic powder by a chemical reaction. Laser beam heating of the powder bed localizes the CVD reaction and enables the formation of shapes via laser beam scanning. By choosing different gas precursors and starting powders, a variety of SALDVI structures with tailored compositions and properties can be produced. Figure 1 shows an example of a 15 layer SALDVI shape made from 20  $\mu\text{m}$  diameter SiC starting powder and tetramethylsilane gas, and the laser scan pattern used to build the part.

SALDVI is a complex process involving the laser heating and localized chemical vapor infiltration of layers of powder. Chemical vapor infiltration of bulk preforms has been experimentally<sup>5-6</sup> and theoretically<sup>7-9</sup> studied in many forms. The infiltration kinetics are difficult to predict and understand theoretically, and depend on the temperature distribution in the preform and on the transport rate of reactants into and products out of the preform. Both of these quantities change continually as the workpiece evolves during infiltration. SALDVI adds the complication of laser heating, where the particle size, particle material, matrix material, gas precursor pressure, laser wavelength, and instantaneous density all contribute to the temperature distribution<sup>10</sup>. The depth of penetration for a given set of SALDVI processing conditions is important in determining the thickness of layers and the mechanism by which adjacent layers bond. In this work the effect of particle size on the laser-induced chemical vapor infiltration of silicon carbide into loose silicon carbide or alumina powder layers is experimentally studied.

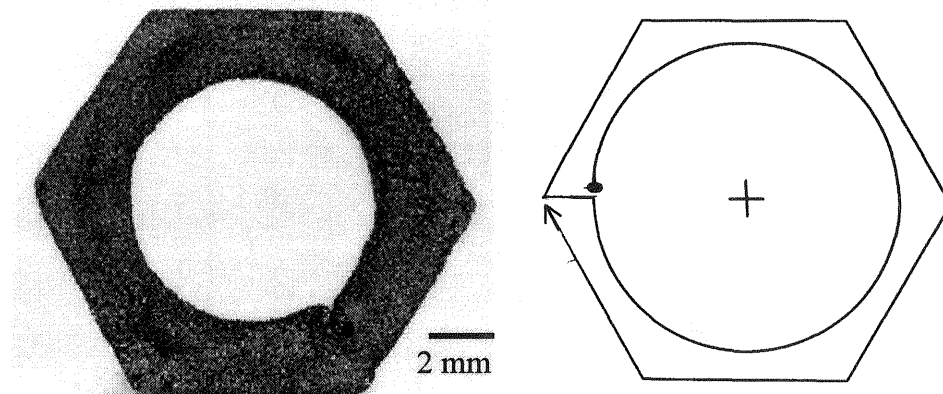


Figure 1. SALDVI SiC 15 layer shape and build pattern.

### Experimental

Three sizes of silicon carbide powder and two sizes of alumina powder were used as starting powders for SALDVI in this study. Each powder was characterized by average size, packing fraction, and transmissivity at the CO<sub>2</sub> laser wavelength (10.64 μm). Average size was determined by optical microscopy. Packing fraction was calculated by measuring the mass of each powder as poured into a cavity of a known volume. Transmissivity is defined as the fraction of incident laser power passing through a layer of powder of a given thickness. Layers of powder ranging in thickness from 25 to 250 μm were spread on a transparent window. A 10 watt, 3.5 mm diameter CO<sub>2</sub> laser beam was directed at each layer, and the amount of power transmitted through the layer was detected by a laser power meter.

The SALDVI workstation consists of a 50 Watt CO<sub>2</sub> laser, a vacuum chamber, a powder delivery system, an xy table with scanning mirrors, and an optical pyrometer, all controlled and automated by a computer. SALDVI experiments are performed in closed loop temperature control mode, where the surface temperature of the laser heated workpiece measured by the pyrometer is used as feedback to adjust the laser power to maintain a constant temperature referred to as the target temperature parameter. SALDVI samples were fabricated for each of the five starting powders using tetramethylsilane, Si(CH<sub>3</sub>)<sub>4</sub>, as the gas precursor for the vapor-deposited SiC matrix. The following processing conditions for each starting powder were fixed: 1 mm beam spot size, 10 Torr Si(CH<sub>3</sub>)<sub>4</sub> gas precursor pressure, and 950 C target temperature parameter. Samples 10 mm in length were fabricated by scanning the laser beam in a single line over a semi-infinite powder bed. The laser beam scan speed was varied from 25 to 800 seconds dwell time to study the time evolution of the infiltration. The samples were mounted in epoxy, cross-sectioned at the mid-length, and polished for microscopic evaluation of the infiltrated regions. Image analysis was used to characterize the infiltration behavior for each experimental condition. Area fractions of the powder, vapor deposited matrix, and porous phases were obtained for different regions on the cross-section in 110 μm by 110 μm frames. By taking a series of frames starting from the free powder surface, the extent of infiltration was mapped as a function of depth into the layer. These measurements were obtained at four different locations along the length of each sample and the average value is reported here.

### Results and Discussion

The powder size and packing fraction results are listed in Table 1. The 7  $\mu\text{m}$  SiC powder forms a less dense powder bed than the two larger SiC powders because of its poor flowability and tendency to agglomerate. The other four powders range in packing fractions from 0.38 to 0.46. The poor flow properties of the 7  $\mu\text{m}$  SiC powder made it difficult to spread thin layers for the transmissivity measurement. The transmissivity results are plotted in Figure 2 for the other four powders as a function of powder layer thickness for the  $\text{CO}_2$  laser wavelength. The measurements show that nearly all of the incident beam is absorbed by the two SiC powders for layers thicker than 100  $\mu\text{m}$ . Only when the powder layer thickness approaches the powder size, essentially a monolayer of powder, does transmission of the beam begin to occur. The  $\text{Al}_2\text{O}_3$  powder showed better transmissivity than the SiC powder, and the larger powder sizes transmit more power than the smaller powders for both materials.

Table 1. Starting powder characteristics:

<u>Particle Size</u>	<u>Packing Fraction</u>
7 $\mu\text{m}$ SiC	0.30
20 $\mu\text{m}$ SiC	0.44
80 $\mu\text{m}$ SiC	0.42
20 $\mu\text{m}$ $\text{Al}_2\text{O}_3$	0.38
100 $\mu\text{m}$ $\text{Al}_2\text{O}_3$	0.46

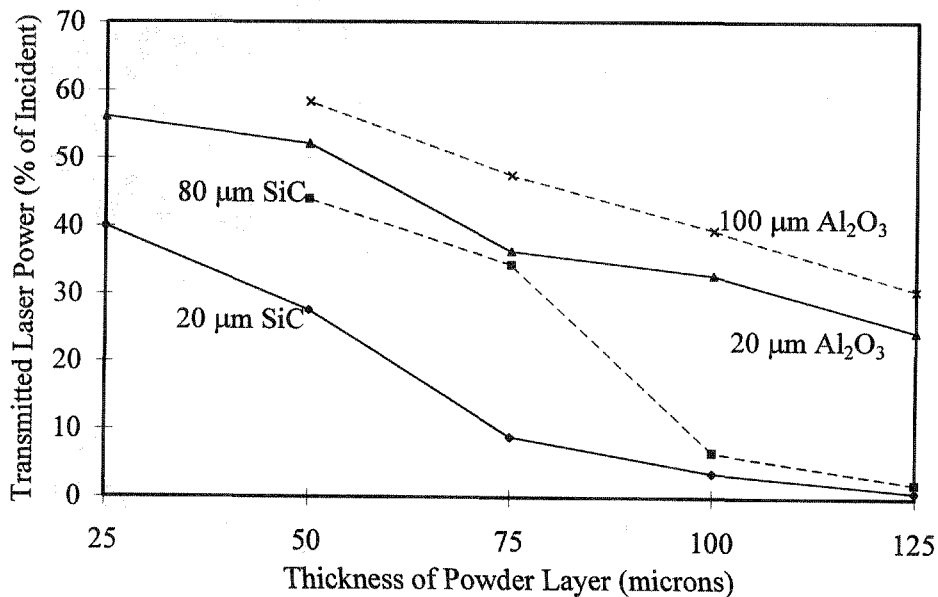


Figure 2. Transmissivity of  $\text{CO}_2$  laser beam vs. powder layer thickness for four SALDVI starting powders.

The cross-sections of SALDVI samples made from the five different starting powders are compared in Figure 3 for a laser beam dwell time of 800 seconds. The cross-sections reveal the presence of three phases in the SALDVI sample: the starting powder particles, the vapor deposited matrix, and uninfiltreated regions or porosity. The distribution of vapor deposited matrix material in the infiltration zone is expected to be a function of two factors: the temperature distribution in the workpiece, and the flux of gas by diffusion into and out of the pore structure. The SiC and Al<sub>2</sub>O<sub>3</sub> starting powders should provide different temperature distributions in the workpiece, while the different powder sizes will yield different scales of pore structure and thus different rates of gas transport. Infiltration occurs most readily at the free surface of the powder and decreases with distance into the powder bed and from the centerline of the scanning laser path. Penetration of the vapor deposited phase appears deepest for the 7 μm SiC powder. The shape of the cross-sections reflects the Gaussian distribution of the power in the laser beam.

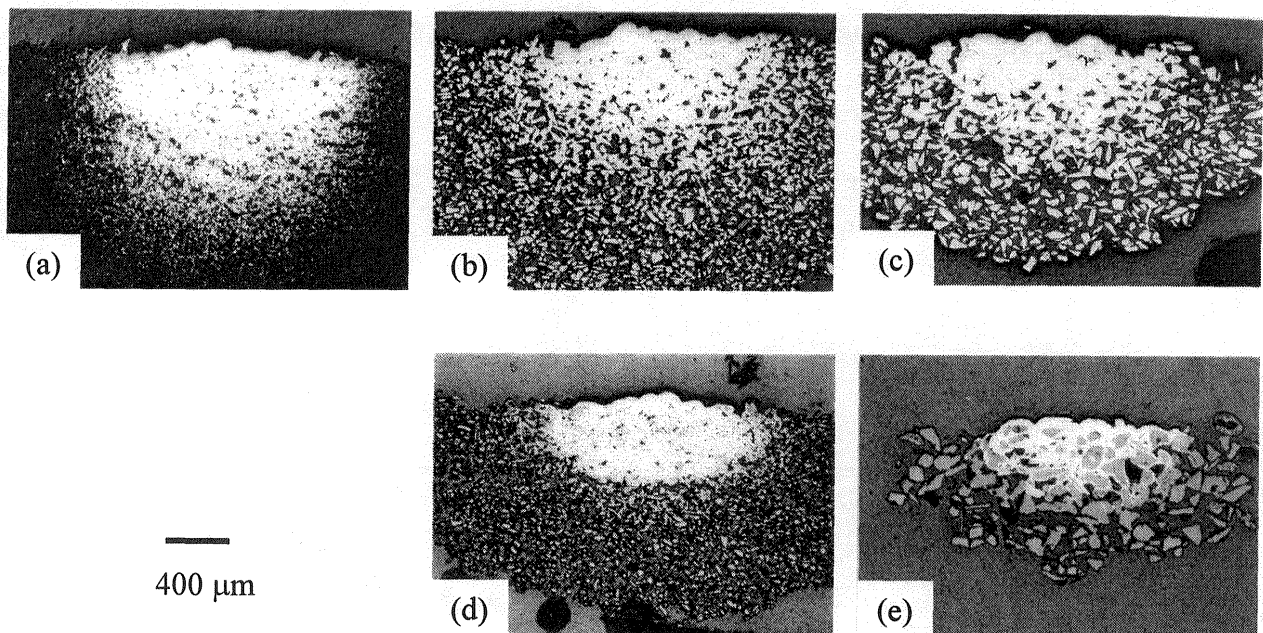


Figure 3. Cross-sections of single line SALDVI samples with starting powders of (a) 7 μm SiC, (b) 20 μm SiC, (c) 80 μm SiC, (d) 20 μm Al<sub>2</sub>O<sub>3</sub>, and (e) 100 μm Al<sub>2</sub>O<sub>3</sub>.

Image analysis was used to quantify the distribution of the porosity in each cross-section. Area fractions of the porous phase were measured as a function of depth from the free surface of the powder layer in 110 by 110 μm frames. Figure 4 shows an example of three such frames used for image analysis for a SALDVI sample made using the 20 μm Al<sub>2</sub>O<sub>3</sub> starting powder. The white regions are the vapor deposited matrix, the gray regions are the starting powder particles, and the black regions are porosity. Figure 5 shows the porous phase area fractions as a function of depth into the sample for samples fabricated from 7 μm SiC powder at four laser dwell times. As the laser heating time increases from 100 to 400 seconds, the infiltrated region extends deeper into the sample. Also, the amount of porosity at a particular location in the sample decreases with increasing heating time. When the dwell time increases to 800 seconds, the infiltrated region continues to extend deeper into the sample. However, the porosity within

the first 250  $\mu\text{m}$  of the surface stays the same, likely due to the presence of trapped porosity. That is, when the infiltration has progressed sufficiently that the pores are no longer interconnected, they become isolated from the bulk gas and vapor deposition within the pore stops. Nevertheless, the areal density in the sample within 250  $\mu\text{m}$  of the surface exceeds 90 % for a powder with an initial packing fraction of 30 %.

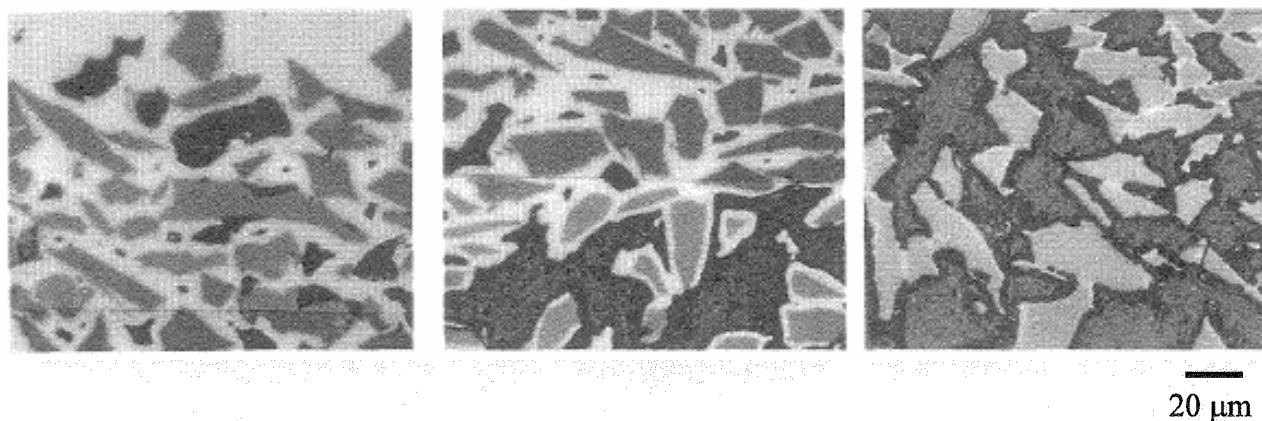


Figure 4. Image analysis frames for 20  $\mu\text{m}$   $\text{Al}_2\text{O}_3$  starting powder at three locations from the free surface of the powder: (a) 0-100  $\mu\text{m}$ , (b) 300-400  $\mu\text{m}$ , and (c) 500-600  $\mu\text{m}$ .

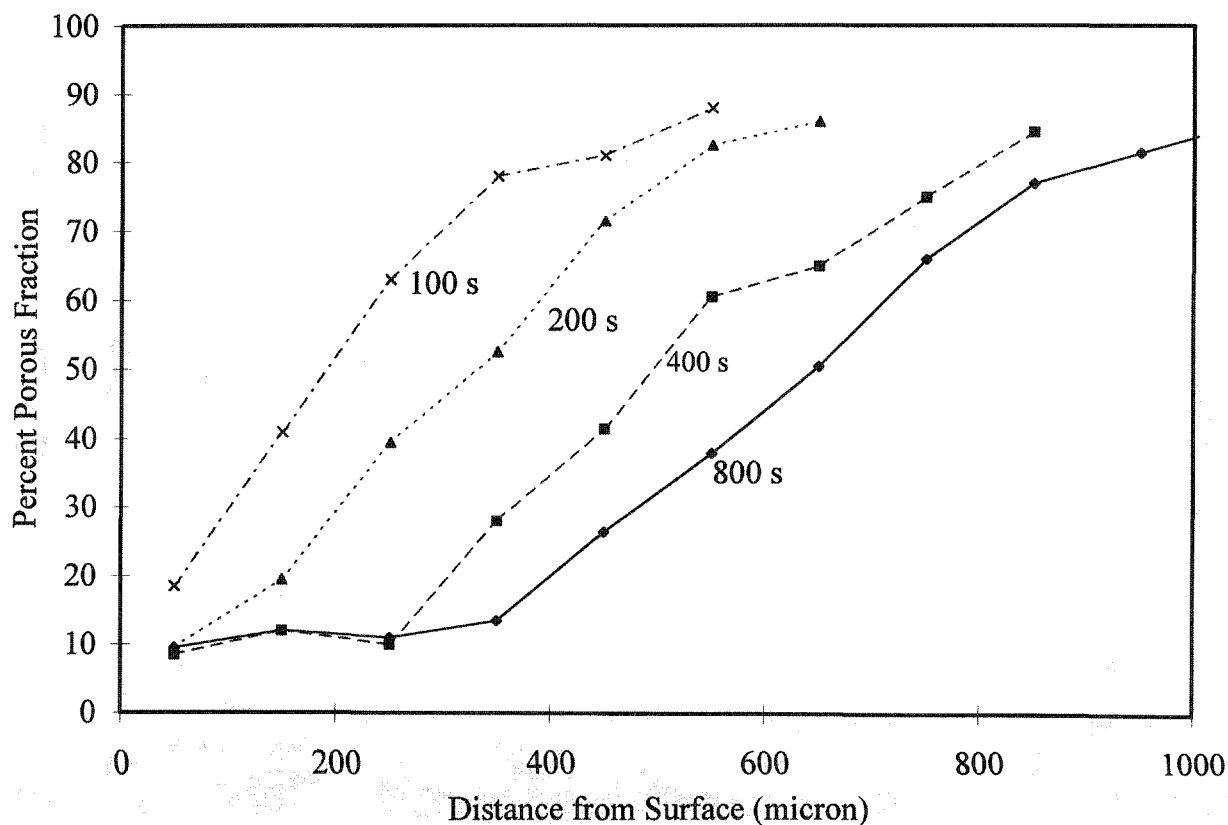


Figure 5. Area fraction porosity vs. distance from free surface of 7  $\mu\text{m}$  SiC starting powder for four laser dwell times.

The porosity distributions in SALDVI samples of the three SiC starting powders and the 20  $\mu\text{m}$   $\text{Al}_2\text{O}_3$  starting powder are compared in Figure 6 for a laser dwell time of 800 seconds. Near the surface, the 20  $\mu\text{m}$  SiC and 20  $\mu\text{m}$   $\text{Al}_2\text{O}_3$  starting powder samples show a slightly higher final density than the 7  $\mu\text{m}$  SiC powder. The final density is the least for the 80  $\mu\text{m}$  SiC powder, due to the presence of large pores between the larger particles in the sample. Comparing the porosity distributions of the SiC samples with the 20  $\mu\text{m}$   $\text{Al}_2\text{O}_3$  sample, the SiC samples show a more diffuse density gradient while the  $\text{Al}_2\text{O}_3$  sample shows a sharper gradient between the infiltrated and uninfiltrated regions. This difference could be explained by considering the difference in thermal conductivity of the two materials. The thermal conductivity of the SiC powder bed is greater than that of the  $\text{Al}_2\text{O}_3$  powder bed, so the temperature distribution would be expected to extend deeper into the SiC powder. Remember that the surface temperature parameter is the same regardless of the starting powder since the incident laser power is varied to yield the same surface temperature parameter as measured by the pyrometer. Also, the result that the  $\text{Al}_2\text{O}_3$  powder transmits the  $\text{CO}_2$  wavelength better than the SiC powder does not greatly affect the depth of the infiltration zone. Toward the later stages of infiltration, the vapor deposited SiC matrix accounts for about 50 volume % of the workpiece and certainly affects its optical behavior since SiC is a strong absorber at the wavelength used in this study. A  $1/e$  extinction length of 9  $\mu\text{m}$  was reported for hot-pressed 6H SiC at a wavelength of 10.6  $\mu\text{m}$ <sup>11</sup>. Therefore, it appears that heat transfer in the SALDVI workpiece using a  $\text{CO}_2$  laser and SiC matrix is by laser heating near the surface and by thermal conduction elsewhere.

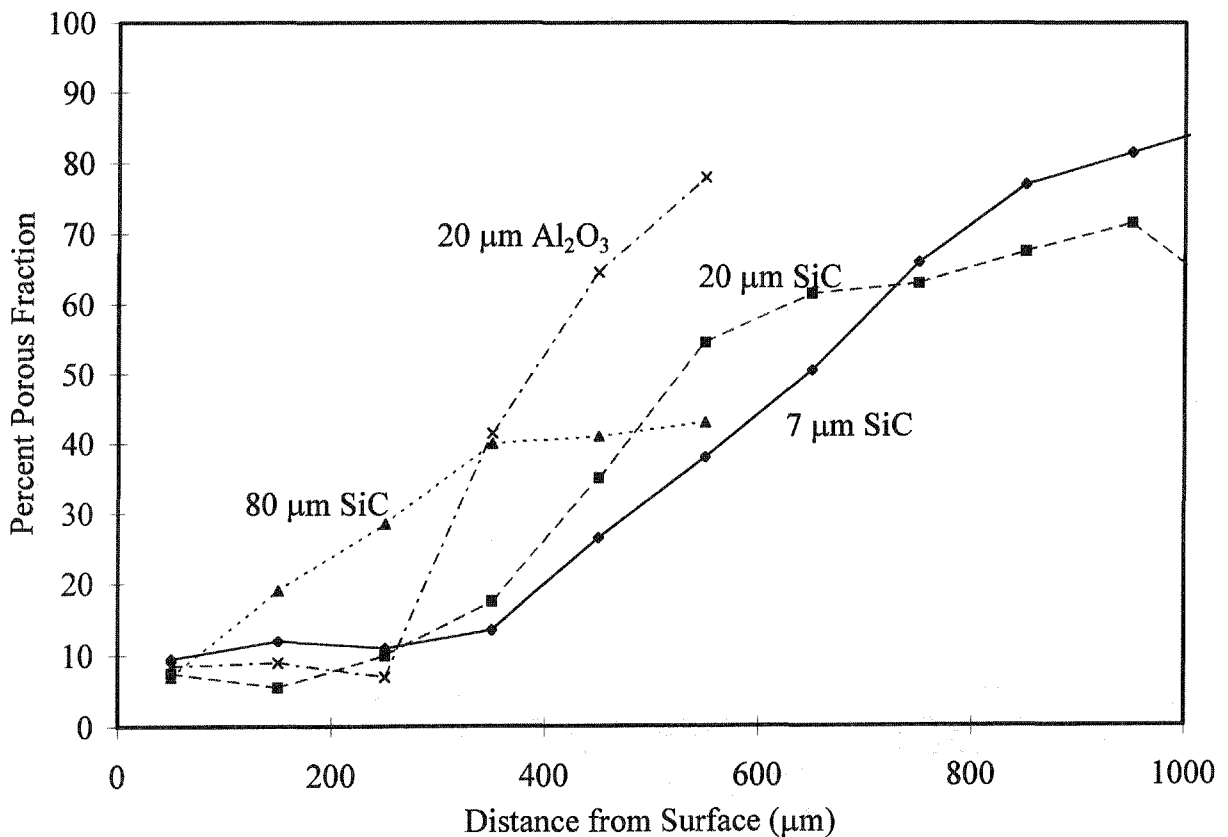


Figure 6. Area fraction porosity vs. distance from free surface for four starting powders at 800 second dwell time.

### Summary

Image analysis was used to quantify the distribution of the various phases in SALDVI samples fabricated from tetramethylsilane gas and several starting powders. Area fractions of the porous phase varied with the powder size and powder material. Solid area fractions of 95 % were measured for samples containing 20  $\mu\text{m}$  particles. Samples with particles over 80  $\mu\text{m}$  contained large pores and lower solid fractions. The thermal conductivity of the starting powders influenced the density gradients. Samples containing starting powders of higher thermal conductivity have a more diffuse infiltration zone than those of the lower thermal conductivity. The transmissivity of the starting powders does not affect the size of the infiltration zone when the vapor deposited matrix material strongly absorbs the incident wavelength.

### Acknowledgements

The authors gratefully acknowledge the support of the Office of Naval Research (grant #N00014-95-1-0978).

### References

1. B.R. Birmingham and H.L. Marcus, "Silicon Carbide Shapes by Selective Area Laser Deposition Vapor Infiltration," Proceedings of the Solid Freeform Fabrication Symposium, The University of Texas at Austin, 1994, pp. 348-355.
2. L. Sun, K.J. Jakubenas, J.E. Crocker, S. Harrison, L. Shaw, and H.L. Marcus, "In-Situ Thermocouples in Macro-Components Fabricated Using SALD and SALDVI Techniques: III. Fabrication and Properties of the SiC/C Thermocouple Device," *Materials and Manufacturing Processes*, **13**, 883-907, 1998.
3. J.E. Crocker, S. Harrison, L. Sun, L.L. Shaw, and H.L. Marcus, "Using SALDVI and SALD with Multi-Material Structures," *JOM*, **50**, 21-23, December 1998.
4. J.E. Crocker, L. Sun, L.L. Shaw, and H.L. Marcus, "Preparation and Properties of In-Situ Devices Using the SALD and SALDVI Techniques," Proceedings of the Solid Freeform Fabrication Symposium, The University of Texas at Austin, 1998, pp. 543-547.
5. D.P. Stinton, T.M. Besmann, and R.A. Lowden, Advanced Ceramics by Chemical Vapor Deposition Techniques, *Ceramic Bulletin*, Vol. 67, No. 2, 1988, pp. 350-355.
6. K. Sygiyama and K. Yoshida, Pressure Pulsed Chemical Vapour Infiltration of SiC to Two-Dimensional-Tyranno/SiC-C Preforms, *J. Mat. Sci.*, Vol. 30, No. 20, 15 Oct 1995, pp. 5125-5129.
7. Sotirchos and Ofori, "Multidimensional Transport Effects on Forced-Flow CVI," *Ind. Eng. Chem. Res.*, 1997.
8. H-C Chang, T.F. Morse, and B.W. Sheldon, "Minimizing Infiltration Times During Isothermal CVI with MTS," *J. Am. Ceram. Soc.*, **80**, 1805-1811, 1997.
9. S.M. Gupte and J.A. Tsamopoulos, "An Effective Medium Approach for Modeling CVI of Porous Ceramic Materials," *J. Electrochem. Soc.*, vol. 137, no. 5, 1626-1638, 1990.
10. D. Bauerle, *Chemical Processing with Lasers*, (Springer-Verlag Berlin Heidelberg, 1986), pp. 41-48.
11. F. Shaapur and S. Allen, "Infrared Optical Absorptivity and Reflectivity of Hot-pressed SiC," *Applied Optics*, 26:2, January 1987.

